Edge Stability of Small-ELM Regimes in NSTX*

A. Sontag[1], J. Canik[1], R. Maingi[1], J. Manickam[2], P. Snyder[3], R. Bell[2], S. Gerhardt[2], S. Kubota[4], B. LeBlanc[2], T. Osborne[3], K. Tritz[5]

1) Oak Ridge National Laboratory, Oak Ridge, TN, USA
2) Princeton Plasma Physics Laboratory, Princeton, NJ, USA
3) General Atomics, San Diego, CA, USA
4) University of California Los Angeles, Los Angeles, CA, USA
5) John's Hopkins University, Baltimore, MD, USA

Reliable access to H-mode regimes with small ELMs is highly desirable for future large experiments such as ITER to ensure adequate survivability of the first wall [1]. The quiescent H-mode, or QH-mode, observed on DIII-D[2], ASDEX [3], JT-60U [4], and JET [3] is one such operating regime. Access to QH-mode has been linked to the appearance of an MHD instability near the plasma edge called the edge harmonic oscillation, or EHO [5]. The EHO allows access to the QH-mode by providing necessary transport near the edge to stabilize the peeling-ballooning modes responsible for ELMs [6], while maintaining good core confinement inside the pedestal. NSTX has observed transition to a small-ELM operating regime where each ELM has less than a 1% impact on the plasma stored energy [7]. The transition to this regime is correlated with the appearance of low-frequency (<10 kHz) MHD oscillations near the plasma edge that have similar characteristics to the EHO. The EHO is hypothesized to be a saturated low-n kink that is destabilized by rotational shear and is accessed at low density and high rotational shear at the plasma edge [6,8]. This work is focused on determining the characteristics of the observed NSTX instability and understanding the conditions that lead to its destabilization and access to small-ELM operational regimes.

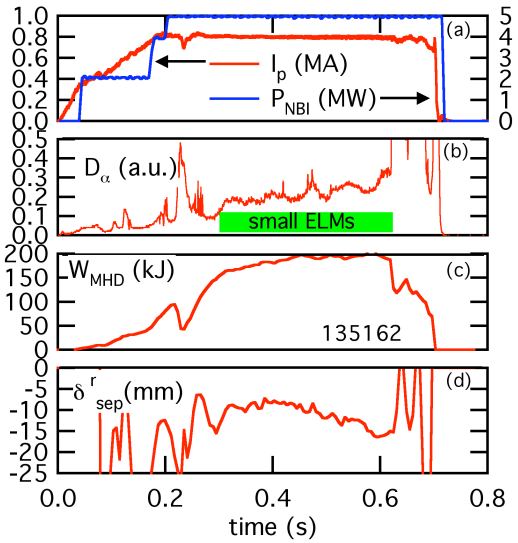

Figure 1: Time evolution of shot 135162

The time evolution of a small-ELM NSTX discharge with this edge instability is shown in Figure 1. In this discharge, the transition to small-ELMs occurs at 0.29 s as shown in the D_α trace in panel (b). These ELMs decrease the plasma stored energy by << 1%, i.e. well below the statistical uncertainty in equilibrium reconstructions. Transition to this regime is associated with a downward biased plasma as

evidenced by δ_r^{sep} < -5 mm, which is consistent with previous observations [7] (δ_r^{sep} is the radial separation of the two separatraces at the outer midplane).

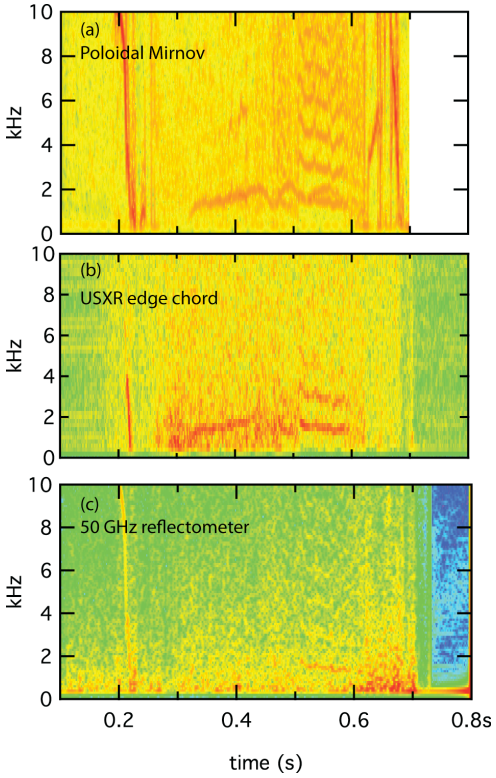

Figure 2: Measurements of an instability near the plasma edge in shot 135162 including (a a) Poloidal Mirnov coil, (b) a USXR chord viewing near the plasma edge, and (c) a reflectometer channel with a cutoff location near the top of the H-mode pedestal.

The edge mode coincident with the transition to small ELMs is observed in the B-dot coils as well as in Ultrasoft X-ray (USXR) emission, as shown in panels (a) and (b) of Figure 2. The channels of the diode array have lines of sight at a single toroidal location that extend from the magnetic axis (channel 1) into the scrapeoff layer (channel 13). The mode is observed as low frequency oscillations that grow in two channels near the plasma edge (channels 11 & 12) starting at approximately 0.29s (coincident with the transition to small-ELMs). These oscillations are coherent with a frequency of 1-3 kHz. This rotation speed is the same as the measured toroidal rotation at the pedestal, indicating an n=1 instability. These oscillations persist throughout the small-ELM period. After 0.5 s, multiple harmonics can be observed with frequencies corresponding to integer multipliers of the lowest frequency mode, which is similar to observations of the EHO in QH-mode. Reflectometer measurements with the cutoff frequency near the top of the pedestal, as shown in Figure 2(c), show density fluctuations at the same frequencies as the observed modes. These fluctuations near the edge are thought to reduce the peeling-ballooning instability drive, thereby decreasing the amplitude of these modes.

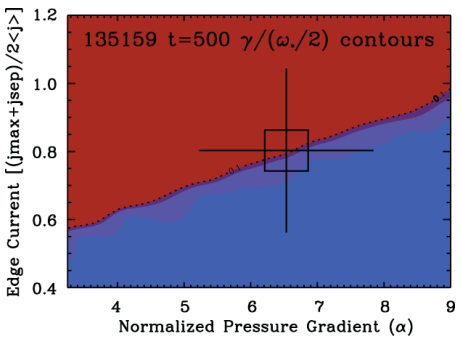

Figure 3: Peeling-ballooning stability of a small-ELM discharge indicating the discharge is on the peeling (current driven) side of stability space.

Ideal MHD stability analysis during the small-ELM phase has been performed using both the ELITE [9] and PEST [10] stability codes. The ELITE analysis was performed using the procedure outlined in [11] with profiles averaged over the entire small-

ELM time. Figure 3 shows the results from the ELITE analysis indicating that the plasma is on the peeling side of the stability limit, with n = 3 being the most unstable mode. The stability boundary of $\gamma/(\omega_*/2) = 0.1$ is consistent with the calculated ELM stability of previous NSTX discharges [12]. Similar calculations for DIII-D show that discharges with the EHO lie near the peeling stability boundary [6]. PEST calculations indicate n = 3-5 are the most unstable modes, with the mode eigenfunctions peaking near the plasma edge. Note that these analyses do not take into account the plasma rotation, which previous calculations have indicated could cause the most unstable mode to shift towards lower-n [6], i.e. closer to observations of a dominant n = 1.

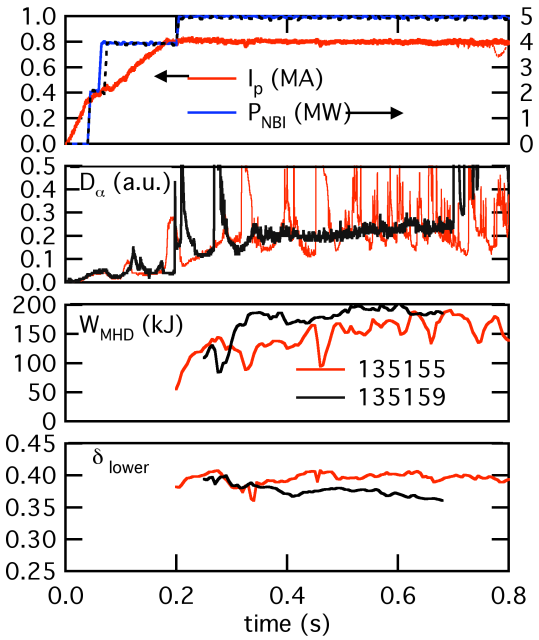

Figure 4: Time evolution of two discharges with similar global plasma parameters but different ELM characteristics. The control shot (red) has large Type I ELMs. The second shot (black) transitions to a small-ELM regime coincident with a programmed change in triangularity at 0.3 s.

A comparison of two shots illustrates the results of operating in a small-ELM regime and gives a possible cause for the transition to this regime. The time evolution for two shots with similar time evolution of global plasma parameters, except for a programmed change in triangularity at 0.3 s, is shown in Figure 4. The control discharge (135155) has large Type I ELMs throughout the discharge, while the second discharge (135159) transitions to a small-ELM regime soon after the decrease in triangularity. The edge MHD instability is observed in the small-ELM discharge but not in the control discharge. The edge electron pressure and pressure gradient for these two discharges are shown in Figure 5. The time was chosen to be during the small-ELM time and between ELMs for the control discharge. The small-ELM discharge has a reduced peak pedestal pressure gradient, as seen in Figure 5 (b), and a less distinct pedestal top which is shifted inward by approximately 2 cm, as shown in

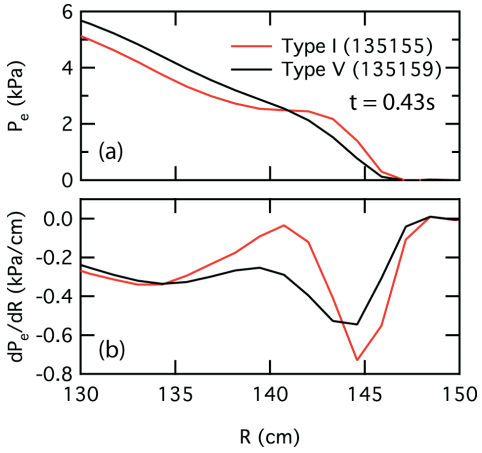

Figure 5: Comparison of (a) electron pressure profile and (b) electron pressure profile gradient for discharges with Type I (red) and Type V (black) ELMs.

Figure 5 (a). A comparison of the edge rotation, rotation shear and collisionality between these two shots is shown in Figure 6. Shot 135155 has slightly increased rotation (Figure 6 (a)) but decreased rotation shear near the top of the pedestal (Figure 6 (b)) as compared to the small-ELM discharge, which is consistent with increased rotation shear resulting in destabilization of the edge mode. Analysis of a larger database of shots shows a wide variation in both rotation and rotation shear at the pedestal for Type I and Type V discharges, so these results are not conclusive. The small-ELM discharge shows increased edge collisionality, consistent with past observations of Type V ELMs as compared to Type I/III ELMing discharges [7]. Analysis of a larger database of shots indicates that $\nu^* > 1$ at the top of the H-mode pedestal eliminates Type I ELMs in NSTX, leaving only Type V. The Type V discharges also show a trend of increased pedestal pressure as compared to Type I discharges. The peeling mode is an edge-localized, current-driven external kink, and further MHD stability analysis must be performed to determine if the increased pedestal collisionality is required to reduce the pressure-driven current near the edge to stabilize the peeling mode. The general trend of increased pedestal pressure in Type V ELMing discharges is suggestive of a pressure driven internal kink that saturates as the mode grows and decreases the edge pressure. However, further analysis is required to determine the destabilization and saturation mechanisms for this edge instability.

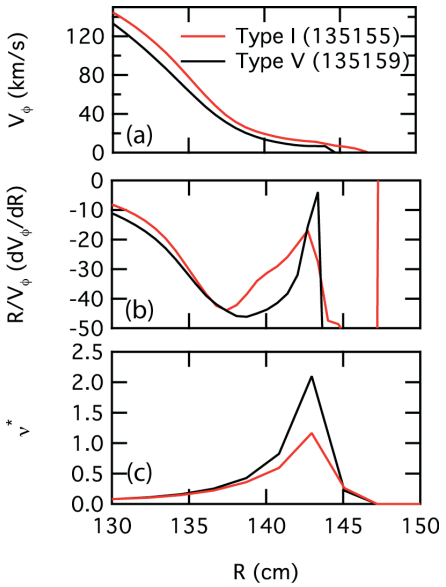

Figure 6: Comparison of (a) toroidal rotation profile, (b) toroidal rotation shear, and (c) normalized collisionality, ν^*, for discharges with Type I (red) and Type V (black) ELMs.

*This work was supported by U.S. DOE Contracts DE-AC05-00OR22725, and DE-AC02-09CH11466

[1] J. Roth, *et. al*., *J. Nucl. Mater*. **1** (2009) 390.
[2] C.M. Greenfield, *et al.*, *Phys. Rev. Lett.* **86** (2001) 4544.
[3] W. Suttrop, *et al., Nucl. Fusion* **45** (2005) 721
[4] Y. Sakamoto *et al., Plasma Phys. Control. Fusion* **46** (2004) A299
[5] K.H. Burrell, *et al.*, *Phys. Plasmas* **8** (2001) 2153.
[6] P.B. Snyder, *et al., Nucl. Fusion* **47** (2007) 961.
[7] R. Maingi, *et al.*, *Nucl. Fusion* **45** (2005) 264.
[8] K.H. Burrell, *et al.*, *Nucl. Fusion* **49** (2009) 085024.
[9] H.R. Wilson, *et al.*, *Phys. Plasmas* **9** (2002) 1277.
[10] Grimm, *et al.*, *Methods of Comp. Phys.* **16** (1976) 253.
[11] P.B. Snyder, *et al., Plasma Phys. Control. Fusion* **46** (2004) A131.
[12] R. Maingi, *et al., Phys. Rev. Lett.* **103** (2009) 075001.